How to cite: *Angew. Chem. Int. Ed.* **2025**, *64*, e202414069
doi.org/10.1002/anie.202414069

Supramolecular Chemistry Hot Paper

'Invisible' Molecular Dynamics Revealed for a Conformationally Chiral π-Stacked Perylene Bisimide Foldamer

*Ben Teichmann, Menyhárt Sárosi, Kazutaka Shoyama, M. A. Niyas, Rajeev K. Dubey, and Frank Würthner**

Dedicated to Professor Pablo Ballester on the occasion of his 65th birthday

Abstract: Whilst energetic and kinetic aspects of folding processes are meanwhile well understood for natural biomacromolecules, the folding dynamics in so far studied artificial foldamer counterparts remain largely unexplored. This is due to the low energy barriers between their conformational isomers that make the dynamic processes undetectable with conventional methods such as UV/Vis absorption, fluorescence, and NMR spectroscopy, making such processes 'invisible'. Here we present an asymmetric perylene bisimide dimer (bis-PBI **1**) that possesses conformational chirality in its folded state. Owing to the large interconversion barrier ($\geq 116\ kJ\ mol^{-1}$), four stereoisomers could be separated and isolated. Since the interconversion between these stereoisomers requires the foldamer to first open and then to re-fold, the transformation of one stereoisomer into others allowed us to 'visualize' the dynamics of folding with time and determine its lifetimes and the energetic barriers associated with the folding process. Supported by quantum chemical calculations, we identified the open structure to be only a fleetingly metastable state of higher energy. Our experimental observation of the kinetics associated with the molecular dynamics in the PBI foldamer advances the fundamental understanding of folding in synthetic foldamers and paves the way for the design of smart functional materials.

[*] B. Teichmann, Dr. M. Sárosi, Dr. K. Shoyama, M. A. Niyas, Dr. R. K. Dubey, Prof. F. Würthner
Institut für Organische Chemie
Universität Würzburg
Am Hubland, 97074 Würzburg, Germany
E-mail: wuerthner@uni-wuerzburg.de
Dr. M. Sárosi, Dr. K. Shoyama, Prof. F. Würthner
Center for Nanosystems Chemistry
Universität Würzburg
Theodor-Boveri-Weg, 97074 Würzburg, Germany

Introduction

The organization of π-conjugated molecules into defined π-stacked structures via self-assembly and folding affords intriguing and specific functions, which are essential to create advanced materials for various applications.[1] However, for the creation of such advanced functional materials, in particular if involving stimuli-responsiveness, the pathways leading to the supramolecular structures and the dynamics of possible transitions in complex supramolecular systems must be better understood.[2] Consequently, the study of self-organization processes via self-assembly pathways has received increasing attention over the past decades[3] for dyes and functional π-systems as these molecules not only offer interesting properties in optoelectronics[4] and photovoltaics[5] but also facilitate the spectroscopic investigation of structural behaviors due to their intriguing optical properties. Interestingly, however, the depth of such studies with regard to folding processes has been far less explored.[6]

One promising chromophore for such studies is the perylene bis(dicarboximide) (PBI), renowned for its photothermal robustness, high tinctorial strength, and pronounced π–π-stacking properties.[5b,7] In the last two decades, π–π-stacking of PBIs has been intensively studied both with regard to the preferential packing arrangements and the concomitant (photo-)functional properties[8] and, as a result, it has even been possible to create outstanding materials for organic electronics, photovoltaics, batteries and capacitors based on PBIs.[5a,9] Recently, PBI dyes were also already covalently connected with several linkers to form PBI foldamers that are dynamic and show stimuli-responsive folding (e.g. solvent, temperature, light, and additive).[10] π–π-stacking of PBI units in such foldamers does not depend on a high concentration as thermodynamic driving force to trigger self-assembly, making them next-generation molecules for stimuli-responsive and adaptive materials.[11] However, despite of an improved understanding of dye–dye interactions, especially for the PBI family, we are far from fully comprehending the complex molecular dynamics in such foldamers due to the complex interplay of kinetics and thermodynamics.[12] Accordingly, in previous research, several foldamers were approximated to a two-state model—an open and closed form—to allow for a simple thermodynamic treatment.[13] Thus, although multiple conformations were likely to co-exist, low kinetic barrier and fast interconversion

at equilibrium made the identification of such conformers in PBI foldamers until now 'invisible' to conventional spectroscopic measurements such as UV/Vis absorption, NMR, and fluorescence spectroscopy.[10b,13,14]

Our continued interest in PBI aggregates and covalently connected PBI oligomers led us now to design a showcase example based on an asymmetric PBI folda-dimer (bis-PBI **1**, Figure 1a) that can fold into multiple conformers and exhibits intriguing axial/conformational chirality. As we will show in the following, owing to the kinetic stability of multiple conformers, diastereomers and enantiomers could be isolated for bis-PBI **1** by high performance liquid chromatography on a chiral stationary phase (in the following called chiral HPLC). Thereafter, a time-dependent investigation of the isolated conformers by chiral HPLC showed the dynamics of opening and re-folding of bis-PBI **1** which is otherwise 'invisible' at equilibrium. Thus, our work reveals the 'invisible' folding dynamics in foldamer bis-PBI **1**. Herein, a potential energy landscape for the folding process developed from experimental rate constants and theoretical calculations revealed that an open state is only a fleetingly metastable state. These insights obtained for bis-PBI **1** should be useful in the design of next generation adaptive materials.

Results and Discussion

Design and Synthesis of the Dimer

The dimer bis-PBI **1** (Figure 1a) was synthesized as per our recently reported multistep procedure using regioisomerically pure 1,7-di(4-*tert*-butylphenoxy)perylene tetraester as the starting compound (Scheme S1).[15] Following the strategy developed by Matile and co-workers, the two PBI units in the dimer are covalently connected through an *ortho*-methyl-phenyl linker that orients the dimer into an ordered foldamer.[16] Herein, the 1,7-bay-positions of each PBI unit were substituted with 4-*tert*-butylphenoxy groups. This 1,7-functionalization induces asymmetry for the rotationally π-stacked PBI dimer leading to two diastereomers, i.e. (*cisoid*)-**1** and (*transoid*)-**1** (Figure 1a). However, due to the presence of *ortho*-methyl-phenyl linker, additional possible stereoisomers can be envisaged as shown in Figure 1b, due to the axial chirality of linker to the PBI bay-substituents (Figure 1c&d).

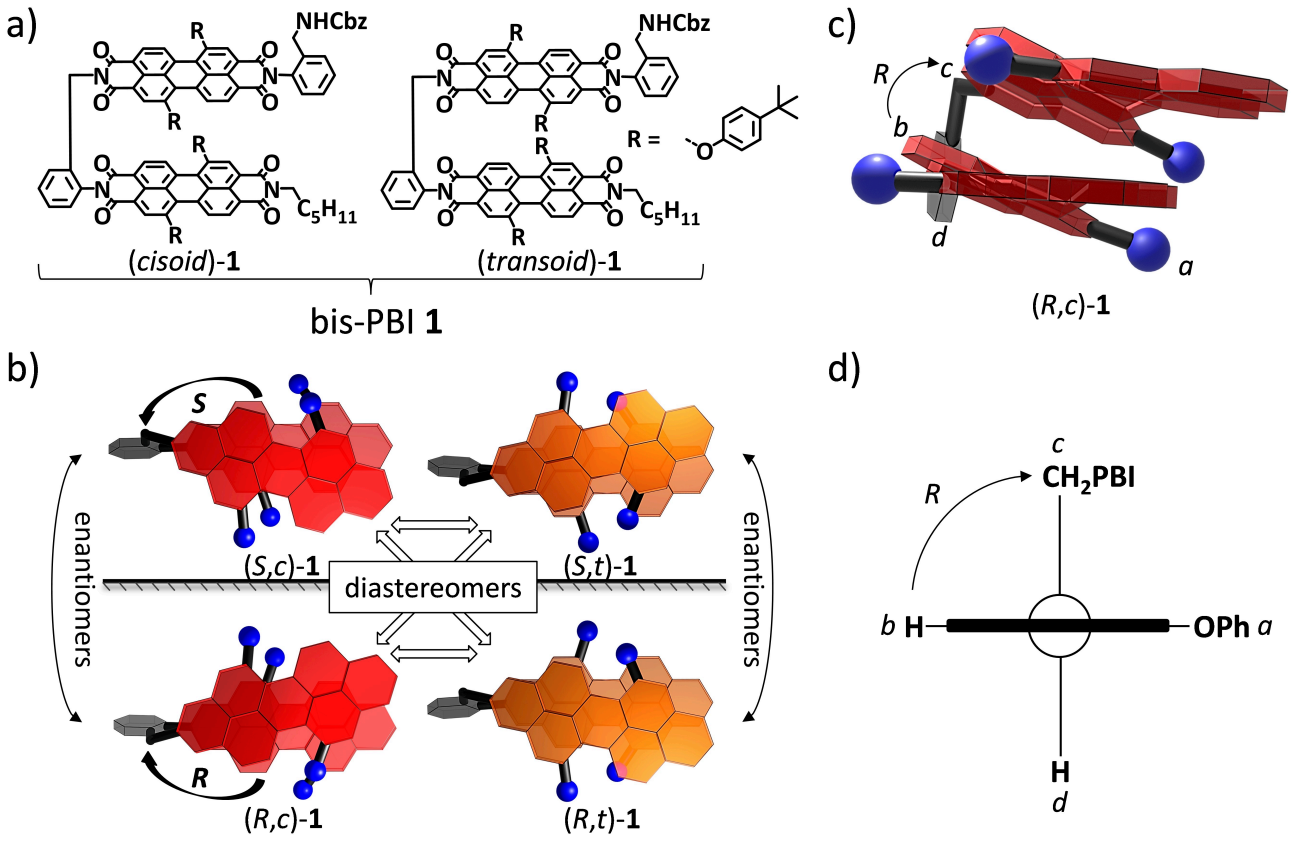

Figure 1. a) Molecular structure of bis-PBI **1** and b) molecular model of the four diastereomers/enantiomers of bis-PBI **1** {(*S*,*c*)-**1** (top left), (*S*,*t*)-**1** (top right), (*R*,*c*)-**1** (bottom left) and (*R*,*t*)-**1** (bottom right)} in closed π-stacked structures. c) Front view of molecular model of (*R*,*c*)-**1** shown with axial chiral priority and d) a schematic representation of the axial chiral *R* alignment from PBI scaffold to linker in (*R*,*c*)-**1**. Cbz: benzyloxycarbonyl.

Separation and Identification of Stereoisomers

After purification of bis-PBI **1** with silica-gel column chromatography followed by size exclusion chromatography and gel permeation chromatography, the ^{1}H NMR spectrum obtained at 295 K in CD_2Cl_2 showed two sets of independent signals in a one-to-one ratio. This was especially visible for the splitting of singlet and doublet signals located at ca. 4.8 and 4.3 ppm, respectively, originating from the aliphatic protons of the benzyloxycarbonyl (Cbz) and benzylamino groups (Figure 2, see the spectra of **ref-PBI** and bis-PBI **1**). This observation indicated the presence of two species, which are in slow exchange at the NMR time scale even at 398 K (Figure S2). Therefore, a sufficiently large barrier between the two species regarding separation was anticipated. Thus, with the help of chiral HPLC, we isolated four different species after multiple cycles (Figure 3). Two sets of isolated species matched the independent signals observed in the ^{1}H NMR (diastereomers, Figure 2) and other two sets of species showed identical ^{1}H NMR signals (enantiomers, Figure 2). Further, circular dichroism (CD) spectroscopy of all four species confirmed that two out of four species are diastereomers (*cisoid* and *transoid*) while the remaining species are enantiomers (*R* and *S*) of bis-PBI **1** (Figure 4b). Comparison of experimental and time-dependent density functional theory (TDDFT) calculated CD signals (Figure 4b & S11 & S12) were used to assign the diastereomers (*cisoid* or *transoid*) and enantiomers (*R* or *S*) to the isolated species. At room temperature, these stereoisomers were found to be reasonably stable and showed very slow decay over several days. Therefore, the single crystal of *rac*-(*cisoid*)-**1**, suitable for X-ray diffraction, could be obtained by slow diffusion of *n*-hexane into the solution of *rac*-(*cisoid*)-**1** in toluene. The obtained X-ray crystal structure further confirmed the structure of *cisoid* diastereomer (Fig-

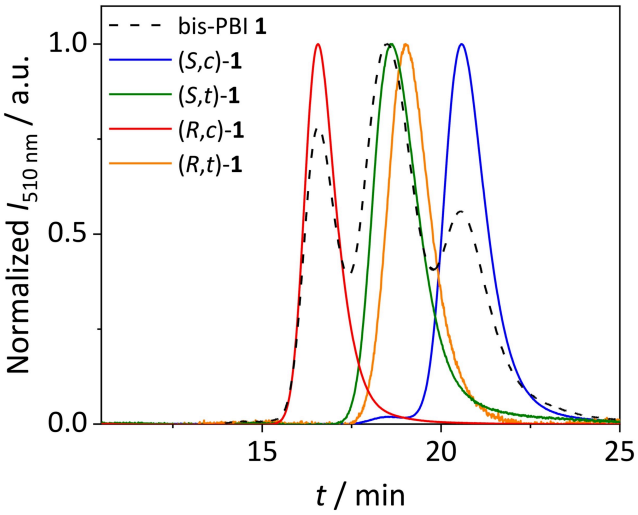

Figure 3. Analytical HPLC of bis-PBI **1** as received from synthesis (dashed line, black) as well as the separated diastereomers, (*S*,*c*)-**1** (blue), (*S*,*t*)-**1** (green), (*R*,*c*)-**1** (red) and (*R*,*t*)-**1** (orange) on a chiral stationary phase (eluent: *n*-hexane/EtOAc = 3/2, *v*/*v*%); flow rate: 1.0 mL min^{-1}; temperature: 295 K; pressure: 1.20 MPa; detector: UV/Vis detector (λ_{mon} = 510 nm).

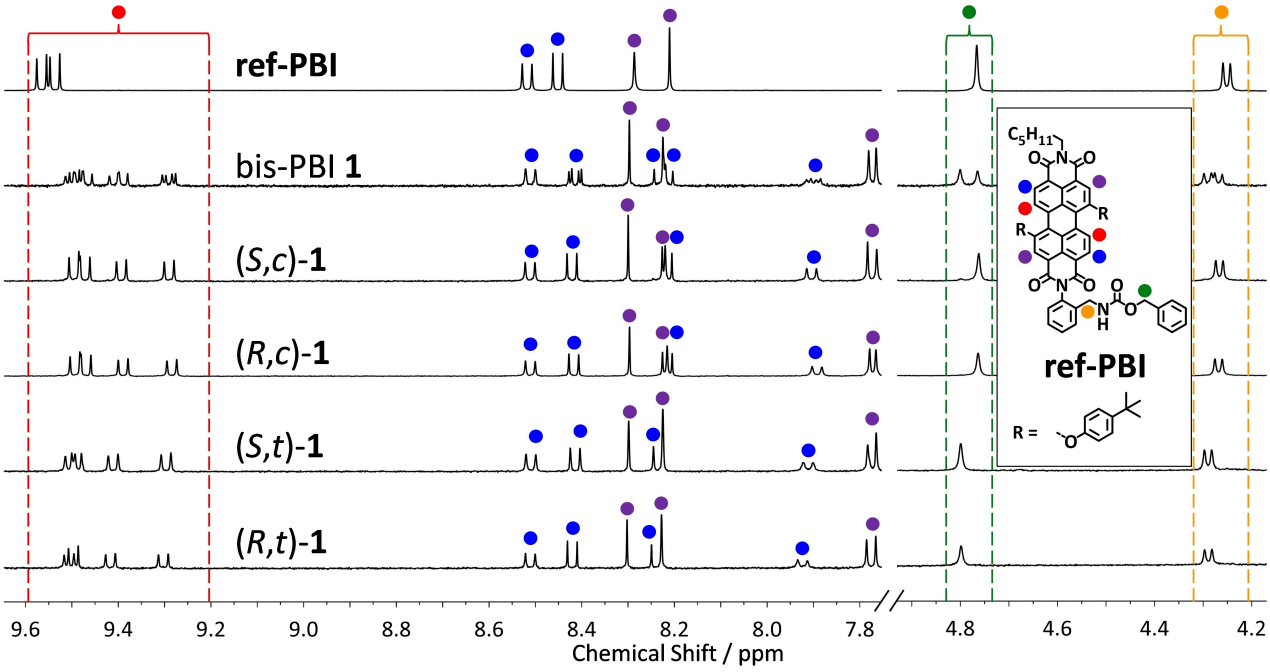

Figure 2. Excerpts of ^{1}H NMR (400 MHz, CD_2Cl_2) spectra from top to bottom of **ref-PBI**, bis-PBI **1** as received from synthesis as well as the separated stereoisomers, (*S*,*c*)-**1**, (*R*,*c*)-**1**, (*S*,*t*)-**1** and (*R*,*t*)-**1** at 295 K with the assignment of the significant proton signals and an inset of the molecular structure of **ref-PBI**.

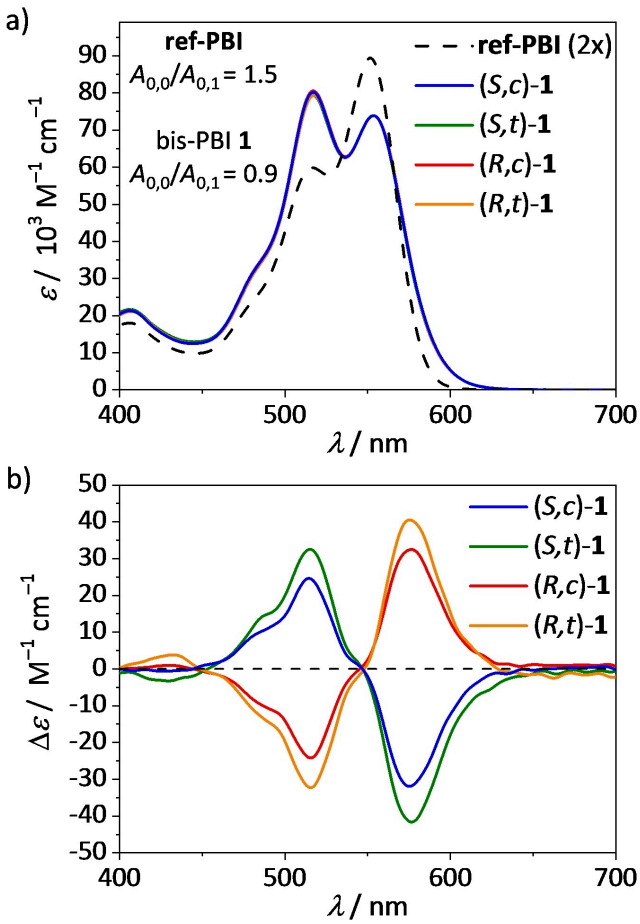

Figure 4. a) UV/Vis absorption (**ref-PBI**—black dotted line—with doubled extinction coefficient, $c = 2.5\times10^{-5}$ M) and b) CD spectra of (*S*,*c*)-**1** (blue, $c = 9.7\times10^{-6}$ M), (*S*,*t*)-**1** (green, $c = 5.6\times10^{-6}$ M), (*R*,*c*)-**1** (red, $c = 9.2\times10^{-6}$ M), and (*R*,*t*)-**1** (orange, $c = 6.3\times10^{-6}$ M) in $CHCl_3$ at 293 K.

ure S8a), whereby the two *cisoid* enantiomers could also be seen as packed in an alternate manner through π–π stacking (Figure S8c). Thus, the four different species isolated are identified as (*R*)-(*cisoid*)-**1** ((*R*,*c*)-**1**), (*S*)-(*cisoid*)-**1** ((*S*,*c*)-**1**), (*S*)-(*transoid*)-**1** ((*S*,*t*)-**1**), and (*R*)-(*transoid*)-**1** ((*R*,*t*)-**1**) (Figure 1b).

Optical and Structural Characterization of Stereoisomers

Once we isolated and identified all four stereoisomers of bis-PBI **1**, optical properties were investigated by UV/Vis absorption, CD, fluorescence, and circularly polarized luminescence (CPL) spectroscopy in $CHCl_3$ at 293 K (Figures 4 & S13). All four conformers of bis-PBI **1** showed very similar UV/Vis absorption and fluorescence spectra indicating the negligible effect of stereoisomerism on the excitonic coupling in the foldamers. On comparison of UV/Vis absorption spectra of bis-PBI **1** with monomeric **ref-PBI** (Figure 2), a clear reversal in the $A_{0,0}/A_{0,1}$ ratio (0.9 for bis-PBI **1** and 1.5 for **ref-PBI**) could be identified (Figure 4a). Such a reversal of $A_{0,0}/A_{0,1}$ ratio from monomeric **ref-PBI** is a hallmark of excitonic coupling in PBIs[17] which thereby confirms the H-type[18] folded state for all four stereoisomers of bis-PBI **1**. Additionally, the density functional theory (DFT) optimized structure of the folded bis-PBI **1** matched an expected H-type coupled structure (Figure S20) confirming that bis-PBI **1** exists as a folded state in solution. The enantiomers of (*cisoid*)-**1** ((*R*,*c*)-**1** & (*S*,*c*)-**1**) and (*transoid*)-**1** ((*S*,*t*)-**1** & (*R*,*t*)-**1**) showed mirror image CD and CPL signals as expected for enantiomers (Figures 4 & S13). However, the diastereomers (*cisoid*)-**1** and (*transoid*)-**1** showed modest differences in the spectroscopic signatures. CD spectroscopy of diastereomers showed that the molar extinction of (*transoid*)-**1** is 25 % more pronounced at the maximum compared to the (*cisoid*)-**1** (Figure 4b). The excitonic Cotton effect observed in the CD spectra further indicates the excitonically coupled nature of the folded conformation of the stereoisomers of bis-PBI **1**. The spectral shape and sign of the Cotton effect are in good agreement with TDDFT calculations (Figures S11 & S12). Further, TDDFT calculations indicate that the helical orientation of the two PBI scaffolds in bis-PBI **1** (providing excitonic chirality) determines the intensity and sign of the CD signal (Figure S21, for further information see SI). CPL spectra are noisy and broad but still revealed a slight difference among the diastereomers in line with CD spectra. From CD and CPL spectroscopy of diastereomers, g_{abs} and g_{lum} values were both calculated to be ±0.001 at the maxima (Figure S14) which is comparable to related chiral PBIs.[19]

Spectroscopic and Theoretical Investigation of Folding Dynamics of bis-PBI 1

Steady state spectroscopic characterization of all four stereoisomers of bis-PBI **1** prompted us to understand the dynamics of folding by time and temperature dependent spectroscopic investigations. Upon heating bis-PBI **1** (as equilibrated mixture of all stereoisomers) in tetrachloroethane (TCE) to 353 K and in benzonitrile (BN) to 328 K, we observed only small thermochromic changes (Figure S10). If the foldamer bis-PBI **1** exist in open form at higher temperature, a clear increase in the $A_{0,0}/A_{0,1}$ ratio should have been visible upon increasing the temperature. However, consistent to the reports of several PBI foldamer systems,[14a,16] no equilibrium between an open and a closed conformation was observed for bis-PBI **1**. Nevertheless, if the open structure is only a transition state or a fleetingly metastable state, a continuous and dynamic opening and folding would be possible in these foldamers. However, even if such an opening and re-folding dynamic exist, it would be 'invisible' at equilibrium. Only a far-from-equilibrium system can make the folding dynamics 'visible' using spectroscopic measurements. Here, the separation and isolation of the stereoisomers provided us the opportunity to 'visualize' the opening and re-folding dynamics in bis-PBI **1**.

As the pure stereoisomers are not in thermodynamic equilibrium, we analyzed the transformation of one of them into other species. Thus, we monitored the decay of (*S*,*c*)-**1**

over time at 373 K with a chiral HPLC (Figure 5a). At this temperature pure (*S*,*c*)-**1** transformed back to all four stereoisomers ((*R*,*c*)-**1**+(*S*,*c*)-**1**+(*R*,*t*)-**1**+(*S*,*t*)-**1**) within ~5 h, with a first order rate constant of $k = 2.44\times10^{-5}\ s^{-1}$ in BN (Figure 5b). The time-dependent transformation of pure (*R*,*c*)-**1** probed by chiral HPLC (Figure S15) also yielded a similar rate constant (Figure S16c). Based on Eyring's equation, a stereoisomerization barrier of $\Delta G^{\ddagger} = 116\ kJ\,mol^{-1}$ was evaluated from both experiments. Since an opening and further re-folding is required for pure (*S*,*c*)-**1** to transform into all stereoisomers (without bond breaking), the time-dependent transformation of a single enantiomer into all four stereoisomers of bis-PBI **1** unambiguously proved the opening and closing of a foldamer which is at equilibrium 'invisible' to spectroscopic measurements. To get deeper insights into the folding process, we went on to analyze the rate of formation of individual species by deconvolution of the composite time-dependent HPLC chromatogram (Figure S16) into individual peaks (Figure S17). During stereoisomerization of (*S*,*c*)-**1**, the formation of (*transoid*)-**1** was found to be faster than (*R*,*c*)-**1** (Figure S17b&d). Vice versa, during stereoisomerization of (*R*,*c*)-**1**, the formation of (*transoid*)-**1** was found to be faster than the respective enantiomer (*S*,*c*)-**1** (Figure S17a&c). This indicates that the energetic barrier associated with the formation of (*transoid*)-**1** is smaller than that of the respective (*cisoid*)-**1** enantiomer during the stereoisomerization of (*S*,*c*)-**1** or (*R*,*c*)-**1**. Here, it is important to note that the rate of formation of (*transoid*)-**1** was evaluated as a combination of its enantiomers ((*R*,*t*)-**1**+(*S*,*t*)-**1**) due to its close overlap in HPLC chromatogram (Figure 3) that makes the deconvolution of (*transoid*)-**1** into (*R*,*t*)-**1** and (*S*,*t*)-**1** unreliable. Thus, it is possible that the two enantiomers of (*transoid*)-**1** would form at different rates. To clarify this and create the potential energy landscape of the whole folding process, we performed theoretical calculations based on a combination of semiempirical and DFT methods (see Supporting Information for more information on the theoretical methods used).

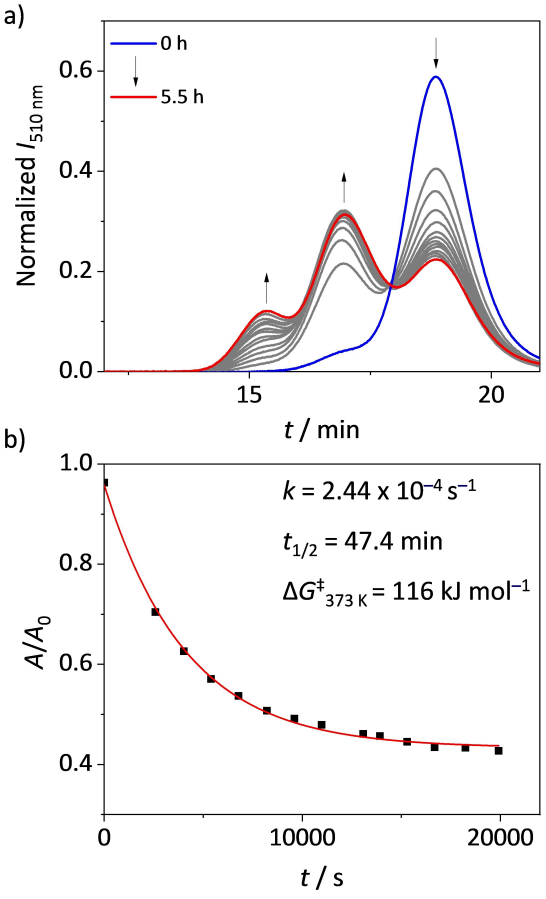

Figure 5. a) Interconversion of (*S*,*c*)-**1** from 0 h (blue) to 5.5 h (red) in benzonitrile (BN) at 373 K by time-dependent analytical chiral HPLC chromatography on a chiral stationary phase (eluent: *n*-hexane/EtOAc = 3/2, *v*/*v*%); flow rate: 1.0 mL min^{-1}; temperature: 295 K; pressure: 1.20 MPa; detector: UV/Vis detector (λ_{mon} = 510 nm). b) The plot of relative concentration of (*S*,*c*)-**1** (symbol) versus time shows the exponential fit for the transformation of (*S*,*c*)-**1** at 373 K in BN from the time-dependent analytical chiral HPLC experiment with the XY fit (red line, see Supporting Information for more information).

Three bond rotations ($\mathbf{C_{ph}}$–$\mathbf{C_{me}}$, **N**–$\mathbf{C_{me}}$, and **N**–$\mathbf{C_{ph}}$) as shown in Figure 6a are involved in the opening and further re-folding of foldamer bis-PBI **1**. A potential energy surface-(PES) scan along all three bond rotations from the folded state shows that the lowest energy bond rotation among the three is along the $\mathbf{C_{ph}}$–$\mathbf{C_{me}}$ bond (Figure S22 & S23). Such a rotation along the $\mathbf{C_{ph}}$–$\mathbf{C_{me}}$ bond allows the foldamer bis-PBI **1** to open. The open structure is a high energy metastable state that would immediately decay to any of the stereoisomers by folding (Figure S23). This re-folding of the open state can proceed with a second rotation along any of the three bonds ($\mathbf{C_{ph}}$–$\mathbf{C_{me}}$, **N**–$\mathbf{C_{me}}$, and **N**–$\mathbf{C_{ph}}$) which then determines the stereochemical fate of the re-folded state. As the first bond rotation ($\mathbf{C_{ph}}$–$\mathbf{C_{me}}$) to open the foldamer is same for all four stereoisomers, a folding pathway that connects the stereoisomers based on the second rotation (**N**–$\mathbf{C_{me}}$ or **N**–$\mathbf{C_{ph}}$) is shown in Figure 6b. For instance, if we start from (*S*,*c*)-**1**, a first bond rotation along $\mathbf{C_{ph}}$–$\mathbf{C_{me}}$ allows bis-PBI **1** to open, followed by a second bond rotation along the **N**–$\mathbf{C_{me}}$ bond, that folds it to (*S*,*t*)-**1**, while if the second rotation is along the **N**–$\mathbf{C_{ph}}$ bond, then (*S*,*c*)-**1** transforms into (*R*,*t*)-**1**. Evaluation of the energetic barrier associated with each of the pathways was done by performing a PES scan along the **N**–$\mathbf{C_{me}}$ and **N**–$\mathbf{C_{ph}}$ bonds at the open state (Figures S24 & S25). PES scans showed that at the open state, the bond rotation along **N**–$\mathbf{C_{me}}$ is lower in energy than along the **N**–$\mathbf{C_{ph}}$ bond. Thus, beginning from a folded state, a $\mathbf{C_{ph}}$–$\mathbf{C_{me}}$ bond rotation to open bis-PBI **1** followed by a second bond rotation along **N**–$\mathbf{C_{me}}$ requires less activation energy than a second bond rotation along **N**–$\mathbf{C_{ph}}$. If we consider the same example as above, starting from (*S*,*c*)-**1**, two consecutive bond rotations along $\mathbf{C_{ph}}$–$\mathbf{C_{me}}$ + **N**–$\mathbf{C_{me}}$ leads to the formation of (*S*,*t*)-**1** which requires lower activation energy (E_a') than forming (*R*,*t*)-**1** by consecutive bond rotations along $\mathbf{C_{ph}}$–$\mathbf{C_{me}}$ + **N**–$\mathbf{C_{ph}}$ ($E_a' < E_a''$). Finally, to reach (*R*,*c*)-**1** from (*S*,*c*)-**1**, two consecutive bond rotations along $\mathbf{C_{ph}}$–$\mathbf{C_{me}}$ + **N**–$\mathbf{C_{ph}}$ are required, corresponding to the higher energetic barrier (E_a''). Thus, quantum chemical

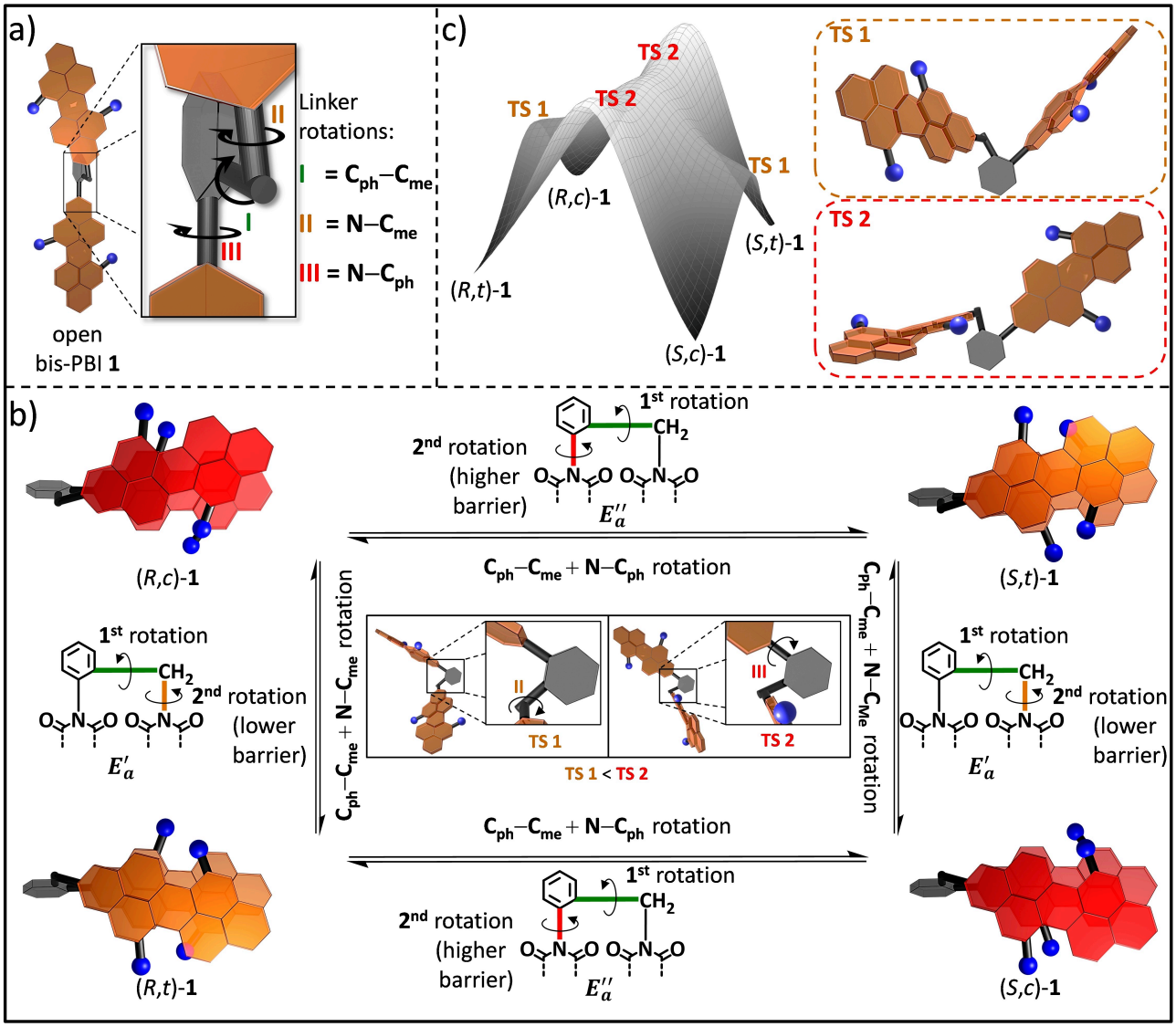

Figure 6. a) Molecular model of bis-PBI **1** in open form and a zoomed in inset of the methyl-phenyl linker showcasing with arrows (black) the possible three rotations C_{ph}–C_{me} (I, green), N–C_{me} (II, orange) and N–C_{ph} (III, red). b) Molecular models of (*S*,*c*)-**1** (bottom right), (*S*,*t*)-**1** (top right), (*R*,*c*)-**1** (top left) and (*R*,*t*)-**1** (bottom left) in closed π-stacked structures with an inset of a proposed molecular model for the transition state (**TS**) structure of the N–C_{me} rotation (**TS 1**, orange) and N–C_{ph} rotation (**TS 2**, red), in addition with the respective enlarged linker benzyl-group, and excerpts of molecular structures with the C_{ph}–C_{me} (green) + N–C_{me} (orange) or C_{ph}–C_{me} (green) + N–C_{ph} (red) rotation highlighted for the respective two activation energies (E_a' and E_a'') for interconversion. c) Qualitative energy landscape of the interconversion process for the four stable conformations of bis-PBI **1** through a meta-stable state with rise of energy (black to grey) and molecular models of the calculated transition states **TS 1** (orange) and **TS 2** (red).

calculations have shown that a pure enantiomer (*S*,*c*)-**1** would transform to (*S*,*t*)-**1** faster than to (*R*,*t*)-**1** or (*R*,*c*)-**1**. Experimental transformation of (*S*,*c*)-**1** into stereoisomers described earlier (see above) showed the formation of (*transoid*)-**1** to be faster than (*R*,*c*)-**1**. Now, in combination with the calculated rotational barriers and the pathway as described in Figure 6b, we can clarify that only one enantiomer of (*transoid*)-**1** forms quickly, which is (*S*,*t*)-**1**. The other enantiomer, (*R*,*t*)-**1**, requires a higher barrier (E_a'') to form from (*S*,*c*)-**1** and thus forms slowly. A qualitative energy landscape was created from both theoretical and experimental results (Figure 6c). The transformation processes described above, as well as the predicted transition states that are visualized in this tent-like energy landscape, showcase the fast transition through the first transition state (**TS 1**) to switch bis-PBI **1** from (*cisoid*)-**1** to (*transoid*)-**1** without changing its axial chirality, i.e. (*S*,*c*)-**1** to (*S*,*t*)-**1**, or (*R*,*c*)-**1** to (*R*,*t*)-**1**. Furthermore, the slower transition through the second transition state (**TS 2**), to generate the respective axial chiral counterparts, enables the foldamer to switch between all four conformations through an open metastable state.

Conclusion

We reported here an asymmetric perylene bisimide foldamer that exists in four stable stereoisomers, i.e. two diastereomers (*cisoid*/*transoid*) and their respective enantiomers (*R*/*S*). Due to the high interconversion barrier ($\geq$ 116 kJ mol^{-1}), we were able to successfully separate and isolate all four stereoisomers. In solution, these isolated pure stereoisomers are in kinetically trapped non-equilibrium states, which decay into all four stereoisomers with time to reach equilibrium. Supported by quantum chemical calculations, we found that the interconversion of one stereoisomer into another require the foldamer to open to a fleetingly metastable state which then re-folds. Thus, the transformation of one enantiomer into other stereoisomers allowed us to observe and monitor the time-dependent opening and re-folding process, which is otherwise 'invisible' in an equilibrated mixture.

We consider the observation of opening and re-folding kinetics to be an important step toward an improved understanding of folding dynamics in synthetic foldamers, which is required to advance the design of new foldamer architectures, and the next-generation stimuli responsive and adaptive materials. In following studies on this or similar systems, we may imagine an annealing strategy in combination with a chiral catalyst to steer the observed molecular dynamics and to create molecular motor systems.

Supporting Information

The data underlying this study is available in the Supporting Information and in Zenodo, an open research repository, at https://doi.org/10.5281/zenodo.12807801. A video is also included in Zenodo to visualize the folding and refolding processes in the presented foldamer.

Acknowledgements

We acknowledge DESY (Hamburg, Germany), a member of the Helmholtz Association HGF, for the provision of experimental facilities. Parts of this research were carried out at PETRA III and we would like to thank Dr. Helena Taberman for assistance in using P11. Beamtime was allocated for proposal I-20220939. The CPL/CD hybrid spectrometer was funded by the Deutsche Forschungsgemeinschaft (DFG, German Research Foundation, project no. 444286426). Open Access funding enabled and organized by Projekt DEAL.

Conflict of Interest

The authors declare no conflict of interest.

Data Availability Statement

X-ray crystallographic data are available free of charge from the Cambridge Crystallographic Data Centre under the reference number CCDC 2371493 via https://www.ccdc.cam.ac.uk/structures/. Additional data supporting the findings are contained in the main text or the Supporting Information. All source files are openly available in Zenodo open research repository at https://doi.org/10.5281/zenodo.12807801

Keywords: chirality · dyes/pigments · foldamers · molecular dynamics · perylene bis(dicarboximide)

[1] a) D. Hu, J. Yu, K. Wong, B. Bagchi, P. J. Rossky, P. F. Barbara, *Nature* **2000**, *405*, 1030; b) R. Bhosale, J. Míšek, N. Sakai, S. Matile, *Chem. Soc. Rev.* **2010**, *39*, 138; c) G. Guichard, I. Huc, *Chem. Commun.* **2011**, *47*, 5933.

[2] a) E. Moulin, L. Faour, C. C. Carmona-Vargas, N. Giuseppone, *Adv. Mater.* **2020**, *32*, 1906036; b) C. D. Jones, J. W. Steed, *Chem. Soc. Rev.* **2016**, *45*, 6546; c) F. Xu, B. L. Feringa, *Adv. Mater.* **2023**, *35*, 2204413.

[3] a) S. Yagai, *Bull. Chem. Soc. Jpn.* **2015**, *88*, 28; b) S. S. Babu, V. K. Praveen, A. Ajayaghosh, *Chem. Rev.* **2014**, *114*, 1973; c) J. Matern, Y. Dorca, L. Sánchez, G. Fernández, *Angew. Chem. Int. Ed.* **2019**, *58*, 16730; d) J. Matern, Y. Dorca, L. Sánchez, G. Fernández, *Angew. Chem.* **2019**, *131*, 16884; e) T. Aida, E. Meijer, *Isr. J. Chem.* **2020**, *60*, 33; f) M. Wehner, F. Würthner, *Nat. Chem. Rev.* **2020**, *4*, 38.

[4] J. Gierschner, S. Y. Park, *J. Mater. Chem. C* **2013**, *1*, 5818.

[5] a) J. H. Kim, T. Schembri, D. Bialas, M. Stolte, F. Würthner, *Adv. Mater.* **2022**, *34*, 2104678; b) T. Weil, T. Vosch, J. Hofkens, K. Peneva, K. Müllen, *Angew. Chem. Int. Ed.* **2010**, *49*, 9068; c) T. Weil, T. Vosch, J. Hofkens, K. Peneva, K. Müllen, *Angew. Chem.* **2010**, *122*, 9252.

[6] O. Pattawong, M. Q. Salih, N. T. Rosson, C. M. Beaudry, P. H.-Y. Cheong, *Org. Biomol. Chem.* **2014**, *12*, 3303.

[7] a) A. Nowak-Król, F. Würthner, *Org. Chem. Front.* **2019**, *6*, 1272; b) R. K. Dubey, F. Würthner, *Nat. Chem.* **2023**, *15*, 884.

[8] a) N. J. Hestand, F. C. Spano, *J. Chem. Phys.* **2015**, *143*, 244707; b) F. Würthner, C. R. Saha-Möller, B. Fimmel, S. Ogi, P. Leowanawat, D. Schmidt, *Chem. Rev.* **2016**, *116*, 962; c) R. M. Young, M. R. Wasielewski, *Acc. Chem. Res.* **2020**, *53*, 1957; d) M. Lijina, A. Benny, E. Sebastian, M. Hariharan, *Chem. Soc. Rev.* **2023**, *52*, 6664; e) S. Samanta, D. Chaudhuri, *J. Phys. Chem. Lett.* **2017**, *8*, 3427.

[9] a) M. Gsänger, J. H. Oh, M. Könemann, H. W. Höffken, A. M. Krause, Z. Bao, F. Würthner, *Angew. Chem. Int. Ed.* **2010**, *49*, 740; b) M. Gsänger, J. H. Oh, M. Könemann, H. W. Höffken, A. M. Krause, Z. Bao, F. Würthner, *Angew. Chem.* **2010**, *122*, 653; c) J. C. Russell, V. A. Posey, J. Gray, R. May, D. A. Reed, H. Zhang, L. E. Marbella, M. L. Steigerwald, Y. Yang, X. Roy, *Nat. Mater.* **2021**, *20*, 1136; d) W. Jiang, Z. Wang, *J. Am. Chem. Soc.* **2022**, *144*, 14976.

[10] a) V. Dehm, M. Büchner, J. Seibt, V. Engel, F. Würthner, *Chem. Sci.* **2011**, *2*, 2094; b) J. J. Han, A. D. Shaller, W. Wang, A. D. Q. Li, *J. Am. Chem. Soc.* **2008**, *130*, 6974; c) T. Sakurai, N. Orito, S. Nagano, K. Kato, M. Takata, S. Seki, *Mater. Chem. Front.* **2018**, *2*, 718.

[11] a) A. Walther, *Adv. Mater.* **2020**, *32*, 1905111; b) M. A. Kostiainen, A. Priimagi, J. V. I. Timonen, R. H. A. Ras, M. Sammalkorpi, M. Penttilä, O. Ikkala, M. B. Linder, *Adv. Funct. Mater.* **2024**, 2402097.

[12] a) D. Bialas, E. Kirchner, M. I. S. Röhr, F. Würthner, *J. Am. Chem. Soc.* **2021**, *143*, 4500; b) F. Würthner, *J. Org. Chem.* **2022**, *87*, 1602.
[13] a) A. D. Q. Li, W. Wang, L.-Q. Wang, *Chem. Eur. J.* **2003**, *9*, 4594; b) S. G. Ramkumar, S. Ramakrishnan, *Macromol.* **2010**, *43*, 2307.
[14] a) C. Kaufmann, D. Bialas, M. Stolte, F. Würthner, *J. Am. Chem. Soc.* **2018**, *140*, 9986; b) M. Son, B. Fimmel, V. Dehm, F. Würthner, D. Kim, *ChemPhysChem* **2015**, *16*, 1757; c) W. Wang, L.-S. Li, G. Helms, H.-H. Zhou, A. D. Q. Li, *J. Am. Chem. Soc.* **2003**, *125*, 1120.
[15] B. Teichmann, B. Liu, M. Hirsch, R. K. Dubey, F. Würthner, *Org. Lett.* **2024**, *26*, 5544.
[16] A.-B. Bornhof, A. Bauzá, A. Aster, M. Pupier, A. Frontera, E. Vauthey, N. Sakai, S. Matile, *J. Am. Chem. Soc.* **2018**, *140*, 4884.
[17] S. Kang, T. Kim, Y. Hong, F. Würthner, D. Kim, *J. Am. Chem. Soc.* **2021**, *143*, 9825.
[18] N. J. Hestand, F. C. Spano, *J. Chem. Phys.* **2015**, *143*, 244707.
[19] R. Renner, B. Mahlmeister, O. Anhalt, M. Stolte, F. Würthner, *Chem. Eur. J.* **2021**, *27*, 11997.

Manuscript received: July 25, 2024
Accepted manuscript online: October 9, 2024
Version of record online: November 14, 2024